Phytochemistry, Vol. 28, No. 8, pp. 2191–2195, 1989.
Printed in Great Britain.

0031-9422/89 $3.00+0.00

CYTOTOXIC APORPHINES FROM *ARTABOTRYS UNCINATUS* AND THE STRUCTURE AND STEREOCHEMISTRY OF ARTACINATINE*

YANG-CHANG WU, CHUNG-HSIUNG CHEN, TSANG-HSIUNG YANG,† SHENG-TEH LU,‡ DONALD R. MCPHAIL,§ ANDREW T. MCPHAIL§¶ and KUO-HSIUNG LEE¶

Natural Products Laboratory, Division of Medicinal Chemistry and Natural Products, School of Pharmacy, University of North Carolina, Chapel Hill, NC 27599, U.S.A.; †School of Pharmacy, Taipei Medical College, Taipei, Taiwan, Republic of China; ‡School of Pharmacy, Kaohsiung Medical College, Kaohsiung, Taiwan, Republic of China; §Department of Chemistry, P.M. Gross Chemical Laboratory, Duke University, Durham, NC 27706, U.S.A.

(*Received in revised form* 21 *December* 1988)

Key Word Index—*Artabotrys uncinatus*; Annonaceae; cytotoxic activity; alkaloids; aporphines; artacinatine; liriodenine; atherospermidine; X-ray crystal structure.

Abstract—The stem and stem bark of *Artabotrys uncinatus* afforded two cytotoxic aporphine alkaloids, liriodenine and atherospermidine, as well as a novel 11-oxoaporphine, artacinatine, which is inactive. The structure of artacinatine was elucidated from spectral data in conjunction with a single-crystal X-ray analysis.

INTRODUCTION

Artabotrys uncinatus (Lam.) Merr., is a perennial vine indigenous to the coastal area of southern China and also to the island of Taiwan [1]. The roots of this plant have been used in Chinese folk medicine as an antimalarial agent. Previous studies by Liang [2] reported yingzhaosu A as the main antimalarial constituent. As part of our continuing searches for novel plant antitumour agents, the methanolic extract of stem parts of *A. uncinatus* was found to show significant reproducible *in vitro* activity against tissue culture cells of human KB, A-549 lung carcinoma, and HCT-8 colon tumour, as well as murine P-388 and L-1210 lymphocytic leukaemia. Bioassay-directed fractionation traced the active fractions to alkaloidal components. We report herein on the isolation and characterization of two cytotoxic aporphines, liriodenine (**1**) and atherospermidine (**2**), in addition to the structural elucidation of an inactive aporphinoid, artacinatine (**3**), which represents the first example of a naturally occurring compound containing the 11-oxoaporphine skeleton.

RESULTS AND DISCUSSION

The methanolic extract of stem parts of *A. uncinatus* was fractionated by solvent partitioning followed by *in vitro* KB cell cytotoxicity tests. Further separation and purification by chromatography furnished the principal active components, liriodenine (**1**) and atherospermidine (**2**) in yields of 0.0006 and 0.0003%, respectively.

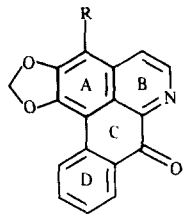

1 R = H
2 R = Me

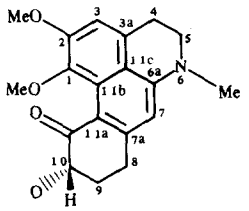

3 R = H
4 R = Ac

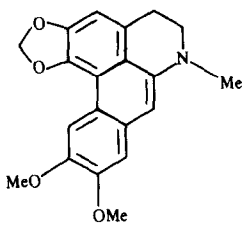

5

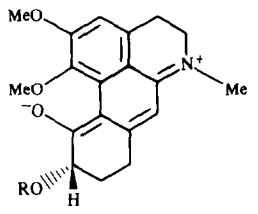

6

The identities of **1** and **2** were confirmed by direct comparison with authentic samples and by spectral analyses. Liriodenine (**1**) [3–6] demonstrated potent cytotoxicity against KB, A-549, HCT-8, P-388, and L-1210 cells with ED_{50} values of 1.00, 0.72, 0.70, 0.57, and 2.33 μg/ml, respectively. This compound has recently been shown to be the main cytotoxic principal in *Thalictrum sessile* [6]. Atherospermidine (**2**) [3–5], with an ED_{50} value of 2.5 μg/ml, was demonstrated for the first time to possess cytotoxic activity against KB cells.

Compound **3**, mp 160–162°, $[\alpha]_D^{24}=0°$, has molecular formula $C_{19}H_{21}NO_4$ as established from high-resolution

*Part 101 in the series 'Antitumor Agents.' For part 100, see L. S. Thurston, Y. Imakura, M. Haruna, D. H. Li, Z. C. Liu, S. Y. Liu, Y. C. Cheng and K. H. Lee, (1989) *J. Med. Chem.* **32**, 604 (1989).

¶Authors to whom correspondence should be addressed.

MS and ^{13}C NMR spectral data. The UV spectrum contained maxima at 214, 261, 290(sh), 344(sh) and 382 (log ε5.03, 4.92, 4.55, 4.43, and 4.79, respectively) nm, suggesting that **3** contained a 1,2-disubstituted dehydroaporphine in conjugation with a keto chromophore. The IR spectrum indicated the presence of a hydroxy group (3415 cm^{-1}) and a conjugated ketone (1650 cm^{-1}). Further support for the existence of a hydroxy group in **3** was provided by the formation of a monoacetate (**4**) and the appearance of an $[M-18]^+$ ion at *m/z* 309 in the MS (Scheme 1).

The ^1H NMR spectrum of **3** (Table 1) revealed singlets for two methoxy groups (δ3.91 and 3.79), two aromatic protons (δ6.85 and 6.02), and an *N*-methyl group (δ3.04) which appeared at rather low field, reflecting a dehydroaporphine moiety. A doublet of doublets at δ4.64, which shifted downfield to δ5.69 in monoacetate (**4**), was attributed to a proton which was adjacent to a hydroxy function. Moreover, spin-decoupling revealed that this proton was coupled to a pair of methylene protons at δ2.02 and 2.57, which were, in turn, coupled with another pair of methylene protons at δ2.94 and 3.16. A pair of coupled triplets at δ3.41 and 3.09 were ascribed to methylene protons at the 4,5-positions of the dehydroaporphine moiety. Comparison of the ^{13}CNMR spectral data for **3** (Table 2) with those for dehydrodicentrine (**5**) [7] revealed close correspondence between signals for the A/B/C-ring segment of a dehydroaporphine in combination with a hydroxycyclohexenone moiety [8]. For acetate **4**, upfield shifts were noted for the two methylene carbons adjacent to the acetate function. A similar upfield shift for the keto carbon attested to its close proximity to the acetate group. In the mass spectrum of **3**, the base peak at *m/z* 283 reflected loss of a hydroxyethylene moiety associated with fragmentation of ring D (Scheme 1).

Single-crystal X-ray analysis established the complete structure and relative stereochemistry of **3**. The crystal structure was solved by direct methods.* Full-matrix least-squares refinement of atomic positional and thermal parameters converged at $R=0.056$ ($R_w=0.078$)† over 2211 reflections. Final non-hydrogen atom positional parameters are in Table 3. The solid-state conformation of one enantiomer is illustrated in Fig. 1. Bond lengths and angles are provided in Fig. 2. In crystals of **3**, pairs of enantiomers are associated around crystallographic centres of symmetry by a bifurcated hydrogen bond.‡ Other intermolecular separations correspond to normal van der Waals distances.

In order to accommodate non-bonded interactions between ring A and ring C substituents, atoms of the A/C naphthalene system in **3** deviate from a strictly planar arrangement, with distortions in the latter being more severe than in the former. Thus, the mean endocyclic dihedral angle about ring bonds in ring A is 4.6° while in ring C the corresponding value is 9.0°. In the former, the two smallest torsion angles§,‖ [0.1(3)° and 1.9(3)°] occur around the C-1–C-2 and C-3–C-3a bonds and the others are related by an approximate C_2 symmetry axis passing through the midpoints of the C-2–C-3 and C-11b–C-11c bonds, indicating that this ring has some 1,3-diplanar character. Endocyclic torsion angles in ring C are related by a pair of C_2 symmetry axes passing through C-7a and C-11c and through the mid-points of the C-6a–C-7 and C-11a–C-11b bonds; consequently, this ring has a shallow twist-boat form. Relief from severe overcrowding of the C-1 methoxy and C-11-carbonyl oxygen atoms is achieved in part by twisting about both the C-11a–C-11b and C-11–C-11a bonds [torsion angles: C-11–C-11a–C-11b–C-1 = 33.6(3)°, O-18–C-11–C-11a–C-11b = 25.4(4)°] to yield an O-12 . . . O-18 distance of 2.753(2) Å.

Table 1. ^1H NMR spectral data for compounds **3** and **4** ($CDCl_3$, TMS as int. standard)

H	**3**(250 MHz)	**4**(400 MHz)
1-OMe	3.79 *s*	3.82 *s*
2-OMe	3.91 *s*	3.93 *s*
3	6.85 *s*	6.86 *s*
4	3.41 *t*(6.2)	3.43 *t*(6.2)
5	3.09 *t*(6.2)	3.13 *t*(6.2)
N-Me	3.04 *s*	3.06 *s*
7	6.02 *s*	6.03 *s*
8	2.94 *ddd*(16.4, 5.2, 3.3)	3.10 *m*
8	3.16 *m*	
9	2.02 *dddd*(12.5, 12, 12, 5.2)	2.33 *m*
9	2.57 *dddd*(12.5, 6.2, 5.9, 3.3)	2.50 *dddd*(12.6, 5.6, 5.5, 2.1)
10	4.64 *dd*(11.5, 5.9)	5.69 *dd*(10, 5.6)
OAc		2.22 s

Coupling constants (Hz) are given in parentheses.

In the solid-state, aromatic methoxy groups generally prefer an arrangement wherein the methoxy methyl carbon atom lies close to the aromatic ring plane thereby allowing for maximum π-electron delocalization [9–12]. This situation clearly obtains at the C-2-methoxy substituent where the methyl carbon atom, C-15, lies only 0.010 Å from the ring A least-squares plane, and the difference observed between the associated bond angles at C-2 [C-3–C-2–O-14 > C-1–C-2–O-14, Δ = 8.8°] is in accord with expectation which would predict enlargement of the former to minimize non-bonded repulsive H(Me) . . . H(aryl) interaction. In contrast, the carbon of the C-1-methoxy substituent, C-13, which would be intolerably close to O-14 or O-18 in a like coplanar

*Crystallographic calculations were performed on PDP11/44 and MicroVAX II computers by use of the Enraf-Nonius Structure Determination Package incorporating the direct methods program MULTAN11/82.

†$R=\Sigma||F_o|-|F_c||/\Sigma|F_o|$; $R_w=[\Sigma w(|F_o|-|F_c|)^2/\Sigma w|F_o|^2]^{1/2}$.

‡Distances and angles characterizing the hydrogen-bonded interactions follow: O-17–H-17 0.92(4) Å; H-17 . . . O-18 1.99(3) Å, O-17–H-17 . . . O-18 129(3)°; H-17 . . . O-18′ 2.39(3) Å, O-17–H-17 . . . O-18′ 133(2)°, where O-18′ is at equivalent position: $-x, 1-y, -z$.

§Both enantiomers of compound **3** are present in the crystal. For the sake of convenience, all torsion angles cited are for one enantiomer only.

‖Endocyclic torsion angles (ω_{ij}, $\sigma\pm0.2$–0.5°) about bonds between atoms *i* and *j* follow: $\omega_{1,2}$ 0.1, $\omega_{2,3}$ −4.5, $\omega_{3,3a}$ 1.9, $\omega_{3a,11c}$ 5.0, $\omega_{11b,11c}$ −9.3, $\omega_{1,11b}$ 6.8 in ring A; $\omega_{3a,4}$ 23.5, $\omega_{4,5}$ −53.5, $\omega_{5,6}$ 57.2, $\omega_{6,6a}$ −26.9, $\omega_{6a,11c}$ −6.6, $\omega_{3a,11c}$ 7.0 in ring B; $\omega_{6a,7}$ 11.4, $\omega_{7,7a}$ −4.8, $\omega_{7a,11a}$ −8.9, $\omega_{11a,11b}$ 15.7, $\omega_{11b,11c}$ −9.1, $\omega_{6a,11c}$ −4.3 in ring C; $\omega_{7a,8}$ 16.0, $\omega_{8,9}$ −32.3, $\omega_{9,10}$ 48.7, $\omega_{10,11}$ −49.9, $\omega_{11,11a}$ 35.0, $\omega_{7a,11a}$ −18.3 in ring D.

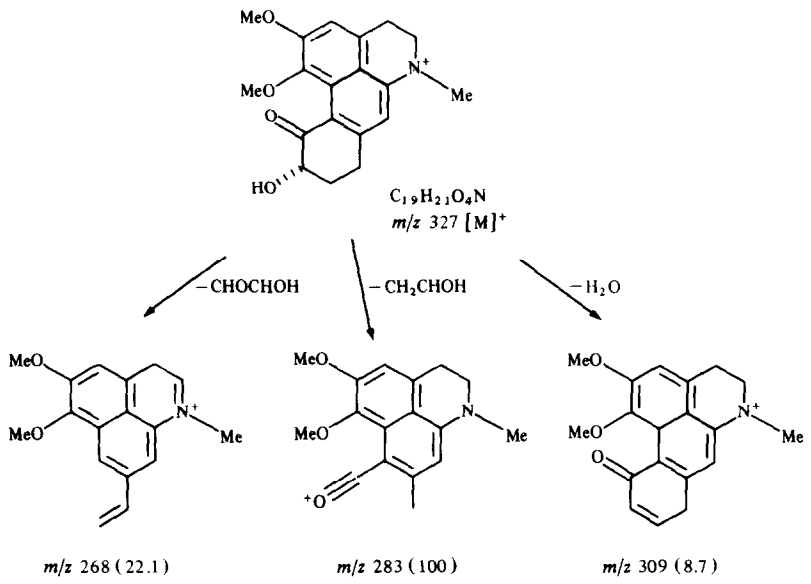

Scheme 1. Mass fragmentation pattern of artacinatine.

Table 2. ^{13}C NMR spectral data for compounds **3** and **4** ($CDCl_3$, TMS as int. standard)

C	3 (100 MHz)	4 (100 MHz)
1	149.43 *s*[a]	149.05 *s*[a]
2	151.61 *s*	151.46 *s*
3	111.18 *d*	111.45 *d*
3a	127.64 *s*[b]	127.64 *s*[b]
4	29.69 *t*	29.68 *t*
5	50.34 *t*	50.42 *t*
6a	142.98 *s*	143.00 *s*
7	101.57 *d*	101.19 *d*
7a	148.79 *s*[a]	146.70 *s*[a]
8	29.58 *t*	28.92 *t*
9	35.71 *t*	30.56 *t*
10	72.75 *d*	74.71 *d*
11	197.70 *s*	191.97 *s*
11a	128.47 *s*[b]	128.25 *s*[b]
11b	115.92 *s*	117.70 *s*
11c	117.43 *s*	117.70 *s*
1-OMe	60.18 *q*	60.12 *q*
2-OMe	56.61 *q*	56.72 *q*
N-Me	39.93 *q*	39.96 *q*
10-AcMe	—	21.17 q
10-AcCO	—	170.42 *s*

The multiplicities were established by DEPT experiments.

[a,b]Assignments with the same superscript may be interchanged.

Table 3. Non-hydrogen atom fractional coordinates and equivalent isotropic thermal parameters for artacinatine (**3**), with estimated standard deviations in parentheses

Atom	*X*	*Y*	*Z*	*B*(Å^2)
C(1)	0.3792(2)	0.2948(2)	0.3121(3)	3.30(5)
C(2)	0.4706(3)	0.3246(2)	0.4665(3)	3.89(5)
C(3)	0.6117(3)	0.3082(2)	0.4644(3)	4.17(6)
C(3a)	0.6656(2)	0.2532(2)	0.3096(3)	3.69(5)
C(4)	0.8186(3)	0.2246(3)	0.3030(4)	4.90(7)
C(5)	0.8450(2)	0.2134(3)	0.1200(4)	4.83(7)
N(6)	0.7731(2)	0.1162(2)	−0.0070(3)	4.44(5)
C(6a)	0.6321(2)	0.1404(2)	−0.0093(3)	3.35(5)
C(7)	0.5426(2)	0.0915(2)	−0.1551(3)	3.59(5)
C(7a)	0.3983(2)	0.1328(2)	−0.1620(3)	3.20(5)
C(8)	0.3087(3)	0.0875(3)	−0.3351(3)	4.25(6)
C(9)	0.1645(3)	0.1663(4)	−0.3522(4)	6.90(10)
C(10)	0.1024(3)	0.2219(4)	−0.1952(4)	6.25(9)
C(11)	0.1981(2)	0.2933(2)	−0.0469(3)	3.79(5)
C(11a)	0.3404(2)	0.2178(2)	−0.0157(3)	3.10(4)
C(11b)	0.4304(2)	0.2466(2)	0.1491(3)	2.98(4)
C(11c)	0.5756(2)	0.2168(2)	0.1505(3)	3.29(5)
O(12)	0.2431(2)	0.2956(2)	0.3137(2)	3.95(4)
C(13)	0.1559(3)	0.4206(3)	0.3905(4)	4.98(7)
O(14)	0.4117(2)	0.3642(2)	0.6185(2)	5.29(5)
C(15)	0.4930(3)	0.4142(3)	0.7798(4)	5.66(8)
C(16)	0.8275(3)	0.0516(3)	−0.1725(4)	5.45(8)
O(17)	−0.0330(2)	0.3012(2)	−0.2112(3)	5.62(5)
O(18)	0.1569(2)	0.4077(2)	0.0319(2)	4.89(5)

arrangement, is displaced very significantly from the same ring A plane, and the associated C-2–C-1–O-12 and C-11b–C-1–O-12 bond angles are less dissimilar [$\Delta = 3.3°$] than those subtended at C-2.

Ring B, with two small adjacent torsion angles [N-6–C-6a–C-11c–C-3a = −6.6(3)°, C-4–C-3a–C-11c–C-6a = 7.0(3)°], approximates to an envelope (half-boat) conformation with C-5 as the out-of-plane atom. At N-6, the mean bond angle is 117.1° and thus the geometry is flattened pyramidal. Contribution from resonance form (**6**) results in an N-6–C-6a bond length of 1.375(3)Å, which is shorter than the lit. [13] mean [1.426(11) Å] for such bonds. This resonance form also results in more nearly equal values for the C-6–C-7, C-7–C-7a, C-7a–C-11 bond

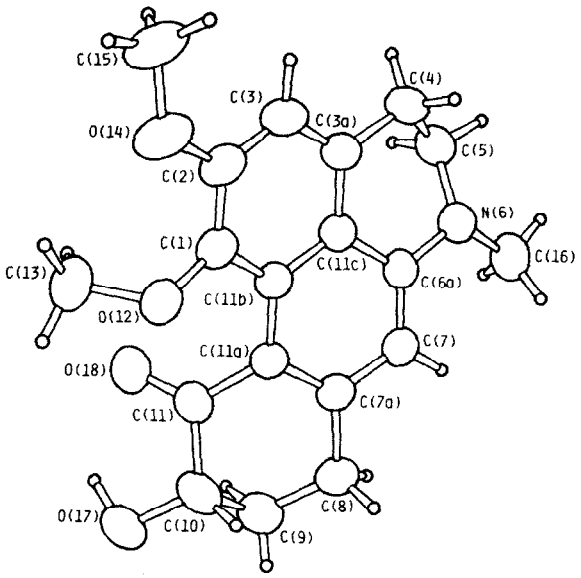

Fig. 1. Structure and solid-state conformation of artacinatine (**3**); small circles represent hydrogen atoms.

lengths [1.381(3), 1.399(3), and 1.395(3) A, respectively] than the corresponding means [1.364(14), 1.406(14), 1.364(14) Å] for similarly disposed bonds in naphthalene rings [13] as well as shortening of the C-11–C-11a distance [1.460(3) Å] from the mean [13] of 1.488(16) Å for a C(ar)–C(=O) bond.

The significant departure of the torsion angle about the C-7a–C-11a double bond [C-8–C-7a–C-11a–C-11 = −18.3(3)°] in ring D from an unstrained value of 0° is a further consequence of molecular distortion to relieve overcrowding of the C-11-carbonyl and C-1-methoxy substituents. Endocyclic torsion angles in this ring are related by an approximate C_s symmetry plane passing through C-7a and C-10, and the ring has a chair conformation considerably flattened around C-7a.

EXPERIMENTAL

Mps: uncorr. ^{1}H and ^{13}C NMR spectra were recorded on Varian XL-400 or Bruker WM-250 spectrometers in appropriate solvents. Chemical shifts are reported in ppm (δ) from TMS as int. standard. Mass spectra were taken at 70 eV using a direct inlet system.

Plant material. A. uncinatus was collected from Chie Shan, Kaohsiung, Taiwan in spring of 1985. A voucher specimen is kept in the School of Pharmacy, Kaohsiung Medical College, Taiwan, Republic of China.

Extraction and isolation. Ground, air-dried stem parts of *A. uncinatus* (3.46 kg) were extracted with MeOH at room temp. The combined extracts (*ca* 84 g) were evapd and partitioned to yield *n*-hexane, $CHCl_3$, and aq. extracts as guided by bioassay in KB cells. The final, active *n*-hexane extract (7.0 g) was chromatographed on a silica gel (350 g, 5 × 40 cm) column using $CHCl_3$–MeOH mixtures of increasing polarity to yield 50 fractions of 100 ml, each of which was monitored by TLC and KB cell bioassay. Further purification of the active fractions 27–34 (45 mg) by column and prep. TLC ($CHCl_3$–MeOH, 5:1) yielded **2** (10 mg), and compound **1** (20 mg) was obtained in a like manner from active fractions 40–44 (56 mg). Chromatography of the $CHCl_3$ extract (40 g) over silica gel (2000 g, 50 × 6 cm), by use of increasingly polar $CHCl_3$–MeOH mixtures, yielded 15 fractions of 500 ml each. Crystallization from Me_2CO of the residue from fractions 9–11 (45 mg) furnished **3** (35 mg).

Liriodenine (**1**). Compound **1** was isolated as microcrystalline yellow needles, mp 286–288° (lit. [14] 282–284°); $[\alpha]_D^{24}$ 0° (MeOH; *c* 0.1), it was identified by direct comparison (mmp, IR, ^{1}H NMR, and TLC) with an authentic sample in our laboratory.

Atherospermidine (**2**). Compound **2** was obtained as fine yellow needles, mp 280–282° (lit. [15] 283–285°), $[\alpha]_D^{24}$ 0° (MeOH; *c* 0.1), it was identified by spectral comparison (IR, UV, and ^{1}H NMR) with lit. [15].

Artacinatine (**3**). Compound **3** was obtained from $CHCl_3$–Me_2CO in the form of greenish prisms, mp 160–162°, $[\alpha]_D^{24}$ 0° (MeOH; *c* 0.1); IR $\nu_{max}^{CHCl_3}$ cm^{-1}: 3435(OH), 1650(ketone), 1589, 1512, 1410, 1297, 1268, 1112, 1065, 1002, 913; UV λ_{max}^{MeOH} nm (log ε): 214 (5.03), 261 (4.92), 290sh (4.55), 344sh (4.43), and 382 (4.79); EIMS 70 eV *m/z* (rel. int.): 328 (10.0), 327[M]$^+$ (51.1), 309[M − H_2O]$^+$ (8.7), 284 (19.4), 283[M − CH_2CHOH]$^+$ (100), 268 (22.1) 222 (5), and 57 (5.5); HRMS: Found, 327.1473, Calcd for $C_{19}H_{21}NO_4$, 327.1471. Acetylation of **3** with Ac_2O–pyridine at room temp. yielded artacinatine acetate (**4**) as a yellow amorphous residue; IR $\nu_{max}^{CHCl_3}$ cm^{-1}: 1730 (ester), 1680 (ketone), 1589, 1511, 1409, 1322, 1313, 1111, 1002; UV λ_{max}^{MeOH} nm (log ε): 218 (5.04), 267 (4.84), 290sh (4.52), 346sh (4.45), and 384 (4.70).

X-Ray analysis of artacinatine (**3**). Crystal data: $C_{19}H_{21}NO_4$, M_r = 327.38, triclinic, a = 10.104(3) Å, b = 10.814(3) Å, c = 8.050(1) Å, α = 107.12(2)°, β = 102.50(2)°, γ = 74.43(2)°, V = 800.7 Å^3, Z = 2, D_{calc} = 1.358 g/cm^3, μ(Cu-Kα radiation, λ = 1.5418 Å) = 7.4 cm^{-1}. Space group $P1(C_1^1)$ or $P\bar{1}(C_i^1)$ from Laue symmetry; shown to be the latter by structure solution and refinement. Sample dimensions: 0.28 × 0.36 × 0.46 mm.

Oscillation and Weissenberg photographs furnished preliminary unit-cell parameters and space group information. Intensity data ($+h, \pm k, \pm l$; θ_{max} = 67°, 3065 non-equivalent reflections) were recorded on an Enraf-Nonius CAD-4 diffractometer (Cu-Kα radiation, incident-beam graphite monochromator; ω–2θ scans). Those 2211 reflections with $I > 3.0\sigma(I)$ were retained for the structure analysis, and the usual Lorentz and polarization corrections were applied. Refined unit-cell parameters were calculated from the diffractometer setting angles for 25 reflections (53 < θ < 65°) widely separated in reciprocal space.

The crystal structure was solved by direct methods, assuming at the outset the $P\bar{1}$ was the correct choice of space group. Initial non-hydrogen atom positions were obtained from an *E*-map. Hydrogen atoms were all located in a difference Fourier synthesis evaluated following several rounds of full-matrix least-squares adjustment of non-hydrogen atom positional and anisotropic temperature factor parameters. With the inclusion of hydrogen atom positional and isotropic thermal parameters as variables (except those at C-9 and C-10, which did not refine to physically acceptable positions) in the subsequent least-squares iterations, the refinement converged (max. shift: esd < 0.03) at R = 0.056 (R_w = 0.078). Final non-hydrogen atom positional parameters are listed in Table 3. A view of the solid-state conformation, with crystallographic numbering scheme, is provided in Fig. 1. Anisotropic temperature factor parameters, hydrogen atom positional and thermal parameters, bond lengths, bond angles, torsion angles, and a list of observed and calculated structure amplitudes have been deposited with the Cambridge Crystallographic Data Centre.

Neutral atom scattering factors used in the structure-factor calculations were taken from lit. [16]. In the least-squares iterations, $\Sigma w\Delta^2[w = 1/\sigma^2(|F_o|), \Delta = (|F_o| - |F_o|)]$ was minimized.

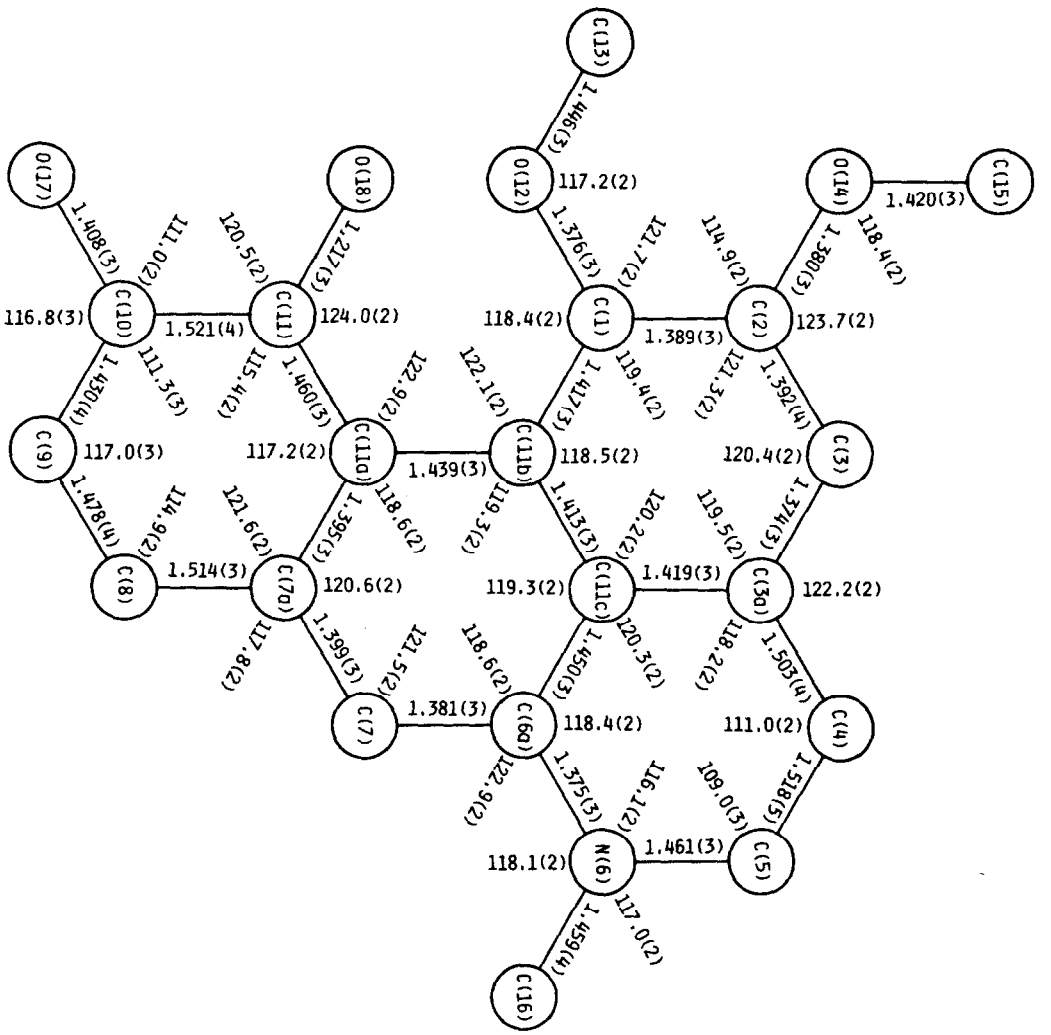

Fig. 2. Interatomic distances (Å) and angles (deg.) in artacinatine (**3**), with estimated standard deviations in parentheses.

Biological evaluation. The cytotoxicity assay was carried out according to a procedure described in ref. [17].

Acknowledgements—This investigation was supported by a grant from the National Cancer Institute (CA 17625) to K. H. Lee.

REFERENCES

1. Li, H. L., Liu, T. S., Huang, T. C., Koyama, T. and DeVol, C. E. (1976) in *Flora of Taiwan* Vol. 6, p. 45. Academic Press, Taiwan.
2. Liang, X. T., Yu, D. Q., Wu, W. I. and Deng, H. C. (1979) *Acta Chim. Sinica* **37**, 215.
3. Guinaudeau, H., Leboeuf, M. and Cave, A. (1975) *J. Nat. Prod.* **38**, 275.
4. Guinaudeau, H., Leboeuf, M. and Cave, A. (1979) *J. Nat. Prod.* **42**, 325.
5. Guinaudeau, H., Leboeuf, M. and Cave, A. (1983) *J. Nat. Prod.* **46**, 761.
6. Wu, Y. C., Lu, S. T., Chang, J. J. and Lee, K. H. (1988) *Phytochemistry* **27**, 1563.
7. Dwuma-Badu, D., Ayim, J. S. K., Mingle, C. A., Tackie, A. N., Slatkin, D. J., Knapp, J. E. and Schiff Jr, P. L. (1975) *Phytochemistry* **14**, 2520.
8. Breitmaier, E. and Voelter, E. (1987) in *Carbon-13 NMR Spectroscopy* p 218. VCH Press, New York.
9. Coggon, P., McPhail, A. T. and Wallwork, S. C. (1970) *J. Chem. Soc. B* 884.
10. Coggon, P., Farrier, D. S., Jeffs, P. W. and McPhail, A. T. (1970) *J. Chem. Soc. B* 1267.
11. Luhan, P. A. and McPhail. A. T. (1972) *J. Chem. Soc. Perkin* II 2006.
12. Luhan, P. A. and McPhail, A. T. (1973) *J. Chem. Soc. Perkin* II 51.
13. Allen, F. H., Kennard, O., Watson, D. G., Brammer, L., Orpen, A. G. and Taylor, R. (1987) *J. Chem. Soc. Perkin Trans. II* S1.
14. Tomita, M. and Kozuka, M. (1965) *J. Pharm. Soc. Jpn* **85**, 77.
15. Harris, W. M. and Geissman, T. A. (1965) *J. Org. Chem.* **30**, 432.
16. *International Tables for X-Ray Crystallography* (1974) Vol. IV. Kynoch Press, Birmingham.
17. Lee, K. H., Lin, Y. M., Wu, T. S., Zhang, D. C., Yamagishi, T., Hayashi, T., Hall, I. H., Chang, J. J., Wu, R. Y. and Yang, T. H. (1988) *Planta Med.* **54**, 308.